

Enhancing Thermal Performance of Cotton Facemasks through the Integration of Phase Change Materials: A Simulation Study

Poptham Chaviengpop^{1,a} and Pimporn Ponpesh^{1,2,b*}

¹Department of Chemical Engineering, Faculty of Engineering, Chulalongkorn University, Bangkok 10330, Thailand

²Control Research Unit, Faculty of Engineering, Chulalongkorn University, Bangkok 10330, Thailand

ABSTRACT

In low temperature regions, people are often exposed to cold air which consumes bodily thermal energy during inhalation and exhalation, resulting in thermal loss from the body. Facemasks could reduce thermal loss. However, at low enough temperatures layering scarves or pieces of clothing on top of facemasks is required to provide adequate insulation against the cold, decreasing the comfort of the users through air pressure loss. Since the COVID-19 pandemic, there has been an increase in mask wearing. Therefore, an improvement of thermal loss reduction onto existing facemasks will grant the users both the benefit of thermal regulation and particulate protection all in one product. To achieve this, there have been suggestions of incorporating phase change materials (PCM) into facemasks to mitigate heat loss throughout the breathing cycle. Although there are some commercially available PCM incorporated facemasks, widespread adoption is limited due to the high cost of prototyping and testing in comparison to facemasks without PCM. Therefore, an investigation of PCM incorporated facemask through computational fluid dynamic (CFD) simulation would provide a low-cost and fast analysis of this technology's thermal performance, solving the problem. In this study, CFD modelling was used to create the model of the PCM incorporated cotton facemask and simulate the mask's thermal behavior under cold environments. The thermal data of inspiration and expiration through the facemask created by the simulation model was successfully validated against a valid numerical model from literature, with the deviation of less than 5.6% and 3.7% for the facemask model with and without PCM, respectively. Furthermore, the inhalation temperature through the PCM incorporated cotton facemask created in this study compared to cotton facemask without PCM is increased by 3.7°C and the exhalation temperature is decreased by 1.2°C, resulting in 2.5 times increase in thermal protection during inhalation and 1.50 times increase in facemask thermal retention during exhalation. The findings of this study will be used to provide manufacturers with an inexpensive and fast method to develop a simulation model of a PCM incorporated facemask that is accurate to reality, thereby reducing the cost of prototyping this technology.

Keyword: Phase change material/ Facemask/ CFD/ Heat transfer

1. INTRODUCTION

In the present, the world is facing severe climate change, causing temperature swings around the world. In areas near the equator and regions sharing the same climate, record low temperatures have been noted down in literature [1]. Exposure to cold environments causes adverse effects on human health. The severity corresponds to how low the body temperature gets. Hypertension, cold injuries, and in severe cases hypothermia can set in. Clothing with high thermal insulation can combat this problem by trapping skin heat radiation from being lost to the atmosphere [2,3]. In current literature, the majority of high thermal insulation clothing optimization is focused on the body, neglecting the respiratory system and the face which is equally important as a significant amount of body heat, 10%, is lost in the respiratory cycle [1,4].

Reported by Habchi et al., the traditional method to protect the respiratory system commonly used is by wrapping a winter scarf around the nostril and mouth. Though if not worn properly, folding cavities can form and enable cold air to directly enter the respiratory system [5]. In comparison, Carnivale et al. suggests that commercial facemasks are as effective as winter scarves in protecting the respiratory system with the advantage of being inexpensive, easier to wear and integrated into cultural norms, especially after the COVID-19 pandemic where facemask adoption is increased [6-8]. However,

*Corresponding Author: Pimporn Ponpesh
E-mail address: *6670180521@student.chula.ac.th, ^bpimporn.p@chula.ac.th

at lower temperatures, a single facemask will not be able to protect the user from cold air. Multiple facemasks or layering other types of clothing on top of the existing facemask will be required with the tradeoff of making breathing more difficult due to the increase in pressure drop through the fabric [9,10]. Alternatively, PCM can be added to the existing facemask to increase protection against cold air.

PCM in the context of industrial applications are materials that are easily able to change phase — with the majority being transitions between liquid and solid — and releases or absorbs a large amount of thermal energy during phase transition [11]. In textile applications, as cold air passes through the fabric, liquid PCM solidifies into solid phase. During the transition, thermal energy is released and heats up the cold air, resulting in comfort for the user [5]. In current literature, most PCMs are incorporated in bodily articles of clothing, especially cotton. However, the problem of this technology lies in the fact that PCM cannot be regenerated this way [5]. Skin heat radiation is not able to melt PCM at a rate fast enough compared to the solidification from the cold environment. Therefore, at steady-state, PCM incorporated clothing will not provide more protection than clothing without PCM [5,12].

In contrast, Habchi et al. and Ghali et al. reported that PCM incorporated within cotton facemasks can be regenerated. After cold air solidifies PCM during inhalation, the solidified PCM can be melted back to liquid during exhalation. The heat from exhalation provides enough heat in a short period of time to effectively melt PCM before the start of the next inhalation cycle, enabling PCM to continuously provide thermal protection [5,12]. Therefore, PCM incorporated facemasks is an interesting avenue for future research.

However, even with such advantages, the application of PCM in facemasks is still scarcely applied commercially. This is due to PCM incorporated fabrics, including facemasks, are significantly more expensive than traditional fabric [13]. Mondal et al. suggested that the increase in cost is due to research and development. Before PCM incorporated fabrics are released into the market, prototyping at different climate conditions needed to be done which uses up capital and time [10]. CFD simulations could be used to overcome this pain point since product modelling and prototyping at several conditions could be done at an extremely fast pace and at a low cost. Therefore, the objective of this research is to prove that CFD simulation model of PCM incorporated cotton facemasks has the capability to accurately simulate the thermal behavior of real PCM incorporated cotton facemasks as a pathway for manufacturers to replace physical prototyping.

2. METHODOLOGY

2.1 Facemask Geometric Model

The drawn cotton facemask geometric model is in the style of plain weave and is created according to Pierce's geometric model. The mathematical equations which relate each geometric structure within the model is listed below [14]:

$$h_j + h_w = D_j + D_w \quad (\text{Eq. 1})$$

$$\frac{h_j}{a_w} = \frac{4}{3}\sqrt{c_j}; \frac{h_w}{a_j} = \frac{4}{3}\sqrt{c_w} \quad (\text{Eq. 2 \& 3})$$

$$a_w = \frac{1}{\text{warp density}} - D_j; a_j = \frac{1}{\text{weft density}} - D_w \quad (\text{Eq. 4 \& 5})$$

$$\theta_j = 212\sqrt{c_j}; \theta_w = 212\sqrt{c_w} \quad (\text{Eq. 6 \& 7})$$

$$c_j = \frac{l_j}{a_w} - 1; c_w = \frac{l_w}{a_j} - 1 \quad (\text{Eq. 8 \& 9})$$

Where; h_j is the warp crimp wave height, h_w is the weft crimp wave height, D_j is the warp yarn diameter, D_w is the weft yarn diameter, a_j is the spacing between warp threads, a_w is the spacing between weft threads, c_j is the warp shrinkage, c_w is the weft shrinkage, θ_j is the warp cover contact

angle, θ_w is the weft cover contact angle, I_j is the warp crimp wave length, and I_w is the weft crimp wave length.

The weft and warp density of the drawn cotton facemask model is 20 and 21 threads per centimeter respectively, resulting in a weft length of 0.5 mm and warp length of 0.4762 mm as shown in Figure 1. The fiber diameter used is 0.263 mm.

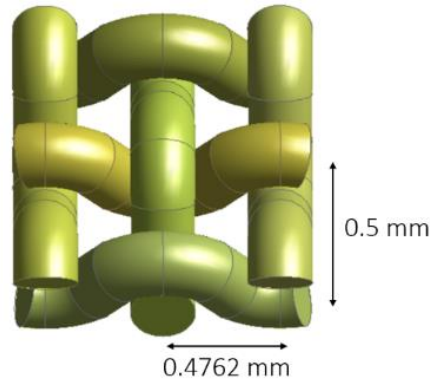


Figure 1. Facemask geometric model

2.2 PCM Incorporated Facemask Geometric Model

PCM is incorporated into the facemask using the random incorporation method, embedding PCM into the facemask randomly. To represent randomness within a volumetric model, the three-node model was used as recommended by Habchi et al. and Ghali et al. [5,12]. The three-node model is shown in Figure 2 [5]. According to the three-node model, PCM will be embedded within two concentric rings — an outer ring and an inner ring — within the cotton fiber.

Due to constraints from overlapping geometry, the PCM is drawn in the shape of a cylinder instead of multiple smaller spheres of the same diameter which is a more accurate representation of PCM embedded within the cotton fiber. There are 9 and 10 PCM cylinders in the outer ring of the warp and weft cotton fibers respectively. The mass fraction of PCM to cotton fiber is 20%, resulting in the calculated PCM cylinder diameter to be 0.04 millimeter. The drawn cross-sectional image of PCM inside a cotton fiber is shown in Figure 3. The side view display is shown in Figure 4. The same boundary conditions mentioned previously will be used to validate the PCM incorporated facemask.

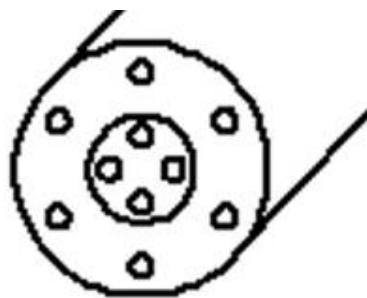


Figure 2. Three-node model diagram [5]

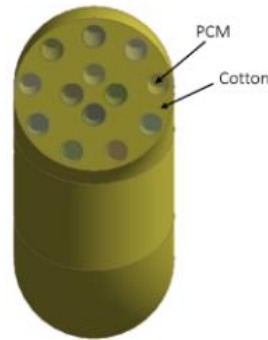


Figure 3. Cross-sectional image of PCM incorporated cotton fiber model

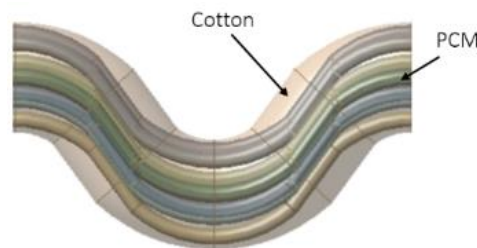


Figure 4. Side profile of PCM incorporation model cotton fiber model

2.3 Fluid Domains

The facemask model is placed within a laminar liquid domain with the same height and width as the facemask model. The domain can be separated into 3 distinct domains which is the interior fluid domain representing the mouth side of the fluid domain, facemask domain representing the volume of and near the facemask, and exterior fluid domain representing the volume outside of the facemask. According to Dbouk et al. [15], the average distance from the mouth to a facemask during usage is 4-14 mm. Therefore, both the interior fluid domain and exterior fluid domain are separated by 4 mm from the facemask domain. Furthermore, numerical verification tests have been done and the chosen minimum mesh resolution for the model is 4 million mesh. The simulation domain is shown in Figure 5.

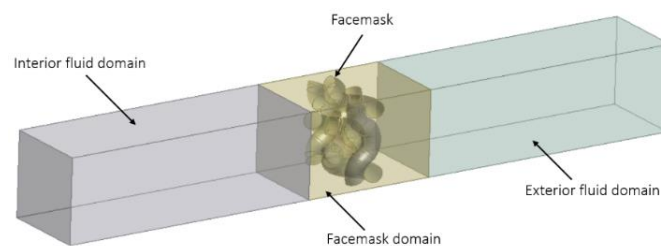


Figure 5. Simulation Domain

2.4 Governing Equations

The following governing equations are for laminar flow in a three-dimensional model without an accelerating reference frame. Conservation of mass, momentum, and energy is included in this study. Furthermore, governing equations relating to solidification/melting are also coupled within the simulation as well.

The equation for the conservation of momentum can be written as:

$$\frac{d}{dt}(\rho\vec{v}) + \nabla \cdot (\rho\vec{v}\vec{v}) = -\nabla p + \nabla \cdot (\bar{\tau}) + \rho\vec{g} + \vec{F} \quad (\text{Eq. 10})$$

Where; p is the static pressure, $\bar{\tau}$ is the stress tensor, $\rho\vec{g}$ is the gravitational body force, \vec{F} is the external body force. \vec{F} arises from interaction with a second dispersed phase or with a porous media. Since the study does not include either of the mentioned models, \vec{F} can be negligible.

The equation for energy conservation and transfer through conduction and convection of fluids (excluding buoyancy-driven flow and radiation) can be written as:

$$\frac{d}{dt}(\rho E) + \nabla \cdot (\vec{v}(\rho E + p)) = \nabla \cdot \left(k_{eff}\nabla T - \sum_j h_j \vec{J}_j + (\bar{\tau}_{eff} \cdot \vec{v}) \right) + S_h \quad (\text{Eq. 11})$$

$$E = h - \frac{p}{\rho} + \frac{v^2}{2} \quad (\text{Eq. 12})$$

$$k_{eff} = k + k_t \quad (\text{Eq. 13})$$

$$h = \sum_j Y_j \vec{J}_j + \frac{p}{\rho} \quad (\text{Eq. 14})$$

$$h_j = \int_{T_{ref}=298.15K}^T c_{p,j} dT \quad (\text{Eq. 15})$$

Where; h is the sensible enthalpy, v is the fluid velocity, k is the thermal conductivity, k_t is the turbulent thermal conductivity defined according to the laminar model, T is the temperature, Y_j is the mass fraction of species j , \vec{J}_j is the diffusion flux of species j , $c_{p,j}$ is the specific heat of species j , and S_h is the defined volumetric heat source.

The energy transport equation in solid regions can be written as:

$$\frac{d}{dt}(\rho h) + \nabla \cdot (\vec{v}\rho h) = \nabla \cdot (k\nabla T) + S_h \quad (\text{Eq. 16})$$

The current model does not include translational or rotational movement of the solid within the simulation domain. Therefore, the second term of the left-hand side of the equation can be negated.

The energy equation for solidification and melting of the PCM is adapted from the energy transport equation in solid regions with an addition of an enthalpy term. The equation can be written as:

$$\frac{d}{dt}(\rho H) + \nabla \cdot (\vec{v}\rho h) = \nabla \cdot (k\nabla T) + S \quad (\text{Eq. 17})$$

$$H = h + \Delta H \quad (\text{Eq. 18})$$

$$\Delta H = \beta L \quad (\text{Eq. 19})$$

$$\beta = \frac{T - T_{solidus}}{T_{liquidus} - T_{solidus}} \text{ if } T_{solidus} < T < T_{liquidus} \quad (\text{Eq. 20})$$

$$\beta = 0 \text{ if } T < T_{solidus}$$

$$\beta = 1 \text{ if } T > T_{liquidus}$$

Where; H is the enthalpy, ΔH is the latent heat, β is the liquid fraction of PCM, L is the total latent heat of the PCM material, and S is the source term.

2.5 Boundary Conditions

Transient simulations were performed using Ansys Fluent 2022 R1 with the Laminar model. The boundary conditions used are specified from research done by Habchi et al. [5]. The boundary conditions are separated into inhalation and exhalation boundary conditions. During inspiration, the velocity inlet is set at the far-right end of the exterior fluid domain plane as shown in Figure 6 with the breathing velocity of 0.802 m/s. The inlet temperature is set at 12°C, representative of cold environmental air. The air will be uniform over the surface of the inlet and is directed through the facemask. The pressure outlet is set to the far-left end of the interior fluid domain. The pressure outlet is specified at atmospheric pressure and is representative of the user's mouth. Inhalation will last for 1.96 seconds after which exhalation will start.

During exhalation, the velocity inlet and pressure outlet will switch places. The velocity inlet will be located at the far-left end of the interior fluid domain and the pressure outlet will be located at the far-right end of the exterior fluid domain as shown in Figure 7. The breathing velocity will be set to 0.802 m/s and the inlet temperature will be set at 33°C, representative of hot exhaled air. Exhalation will last for 2.41 seconds after which the cycle will be completed. Adiabatic conditions and no slip conditions are set to the lateral boundaries of the model, ensuring zero-flux conditions.

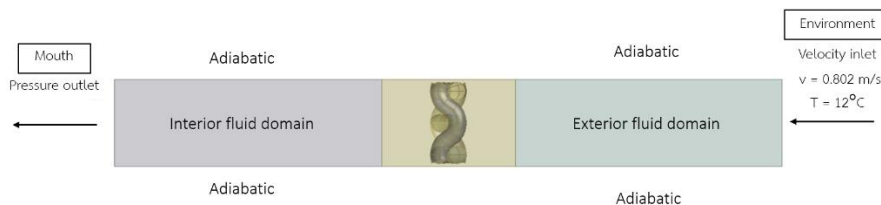


Figure 6. Inhalation boundary condition

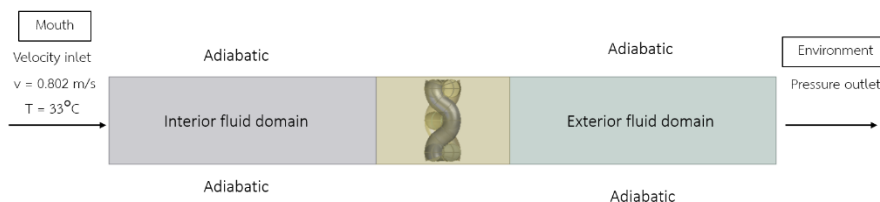


Figure 7. Exhalation boundary condition

3. RESULTS AND DISCUSSION

The data obtained from the CFD model created in this study is validated against the results provided by Habchi et al [5]. In the case of the cotton facemask model without PCM, the air temperature at the outlet during inhalation and exhalation against time is measured in the simulation and compared with data from Habchi et al. As for the cotton facemask model with PCM, both the outlet temperature and liquid fraction of PCM against time is used for validation.

The validation results of the cotton facemask model without PCM produced in this study shown in Figure 8 agree well with the data provided by Habchi et al. with a deviation of less than 5.6%. However, during the start of exhalation, the deviation rises to a peak of 17.9% before decreasing to 2% deviation after 1 second. The discrepancy of the results can be explained by how the transition from inhalation to exhalation is conducted in this study. As the velocity inlet and pressure outlet is swapped during the transition from inhalation to exhalation, the remaining air passing through the mask at the end of the inhalation phase cannot leave the interior liquid domain as the pressure outlet is switched to the side of the exterior liquid domain. The thermal energy from the leftover air at the end of inhalation is compounded with heat from air produced at the start of exhalation, resulting in the detected outlet

temperature at the pressure outlet overpredicting the reference data. After the remaining air from inhalation has been expelled from the liquid domain, the outlet temperature will naturalize back to normal values. This is evident from the outlet temperature agreeing well with the reference data towards the later end of exhalation. Nevertheless, despite the overprediction, the outlet temperature produced in this simulation overall agrees well with data from Habchi et al. Therefore, the cotton facemask model without PCM is considered validated.

From Figure 8, it could be seen that the simulated facemask was able to increase the inhaled temperature to 13.5°C, a 1.5°C difference from the environmental temperature used in this study. The exhaled temperature out of the facemask was reduced from 33°C to 32.2°C. Both results are within 0.6% and 2% deviation from Habchi et al. From the results, it could be seen that wearing normal cotton facemasks provides a slight increase in thermal protection compared to direct breathing. However, normal cotton facemasks do not have a significant gain in reducing heat loss during exhalation.

Cotton Facemask Simulation Outlet Temperature vs Habchi et al. (2014)

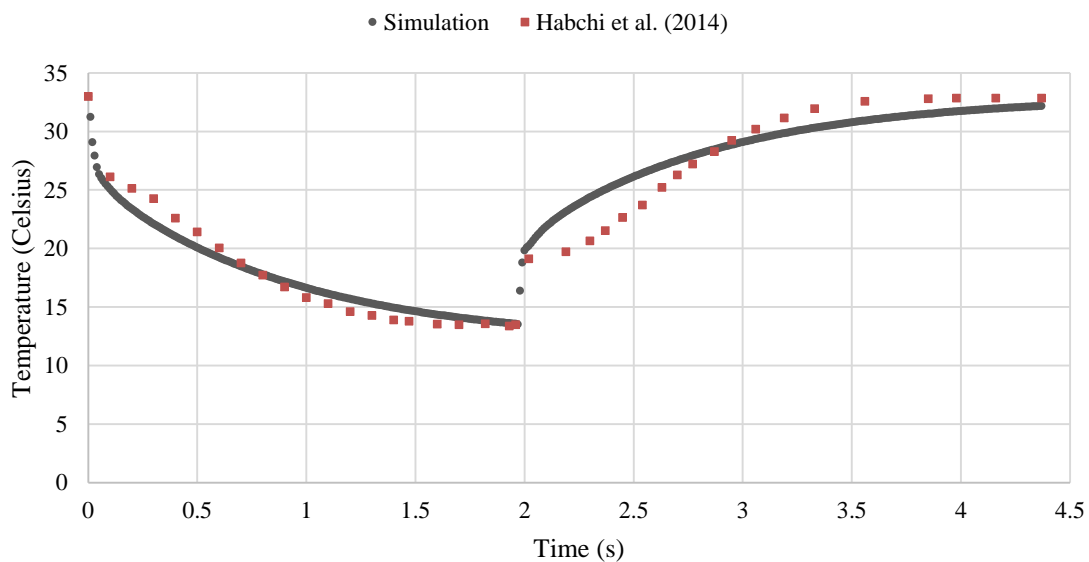


Figure 8. CFD outlet temperature data of cotton facemask compared to data provided by Habchi et al. [5]

The validation results of the cotton facemask model with PCM produced in this study are shown in Figure 9 and Figure 10, displaying the outlet temperature data and liquid fraction of PCM data respectively. From Figure 9, the outlet temperature data throughout both inhalation and exhalation agrees well with the outlet temperature data from Habchi et al. with a deviation of less than 3.7%. However, based on the data from the cotton facemask model without PCM presented in Figure 8, an overprediction in temperature should be present during the first second after exhalation but remarkably is missing in this model as the deviation from the referenced data is reduced in this region compared to that of the model without PCM. This lack of overprediction during the exhalation phase can be explained through the PCM absorbing the excess heat during its phase change. This statement is supported by the graph denoting the liquid fraction of PCM against time shown in Figure 10.

From the liquid fraction data shown in Figure 10, the simulated PCM seem to solidify more slowly than the data provided by Habchi et al. especially after the first second during inhalation. This can be explained by the PCM structure simplification used in this study. PCM structure in this study is a cylindrical shape instead of multiple spheres as used by Habchi et al. Due to the decrease in surface area of cylinders compared to multiple smaller spheres, the rate of solidification is slower. However, the liquid fraction data simulated in this study show an overprediction during most of the exhalation

process. In other words, the PCM in this study melts faster. This can be explained by the excess heat from the outlet temperature during exhalation in this study as shown in Figure 9, which leads to an acceleration in melting of PCM. Nevertheless, the trend of both outlet temperature and liquid fraction behavior of PCM incorporated cotton facemask produced by this study matches closely with data provided by Habchi et al. Therefore, the validation of the cotton facemask model with PCM is also considered successful.

Based on the results simulated from both this study and Habchi et al. [5], it could be seen that adding PCM into cotton facemasks does increase the protection of the respiratory system against cold air. The inhaled temperature is increased to 17.3°C which nets an increase of 5.3°C compared to the environmental temperature and is 3.7°C higher than cotton facemask without PCM, a total of 2.5 times increase in thermal performance. Furthermore, more heat is retained from being lost to the environment as evident by the decrease in outlet temperature out of the facemask during exhalation by 2°C compared to 0.8°C of cotton facemask without PCM, a 1.5 times improvement. Therefore, it can be concluded that PCM does increase the thermal protection of cotton facemasks and retains more heat from exhalation.

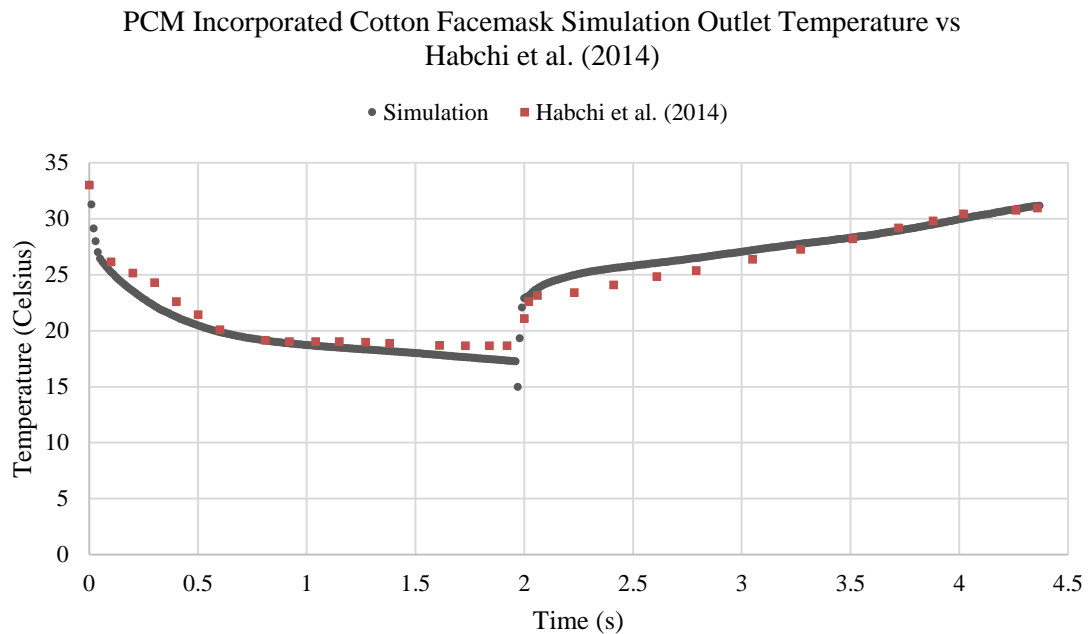


Figure 9. CFD outlet temperature data of PCM incorporated facemask compared to data provided by Habchi et al. [5]

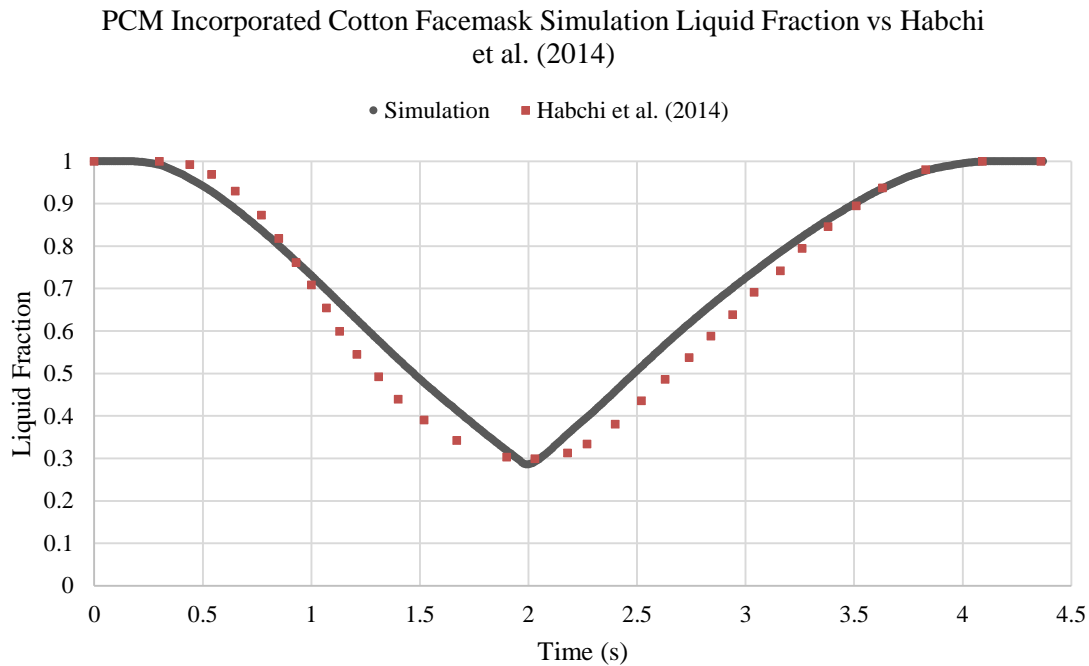


Figure 10. CFD PCM liquid fraction data of PCM incorporated facemask compared to data provided by Habchi et al. [5]

4. CONCLUSIONS

This study was aimed at creating a CFD model that could accurately simulate the thermal behavior of cotton facemasks with and without PCM for manufacturers. The model was validated through the values of outlet temperature and PCM liquid fraction during inhalation and exhalation provided by Habchi et al. The results confirm that CFD model employing Navier-stokes, energy transport, and solidification/melting equations within incompressible flows could predict the thermal behavior of cotton facemasks with the deviation of less than 5.6% and 3.7% for the model with and without PCM, respectively. Though there is an overprediction of the outlet temperature for the cotton facemask without PCM during exhalation and PCM liquid fraction for the cotton facemask with PCM, the simulation was still able to follow the trend closely and provide an accurate thermal data prediction compared to the reference data provided by Habchi et al. The study has confirmed along with the literature that cotton facemasks is able to increase the inhalation temperature by 1.5°C and reduce the exhalation temperature out of the facemask by 0.8°C. Meanwhile, PCM incorporated cotton facemasks can increase the protection of the users' respiratory system against cold air during inhalation and retain more heat within the facemask during exhalation compared to cotton facemasks without PCM. In this study, the inhalation temperature for cotton facemasks with PCM is increased by 5.3°C and exhalation temperature out of the facemask is decreased by 2°C which is 2.5 and 1.5 times improvement compared to cotton facemask without PCM, respectively. In conclusion, PCM incorporated cotton facemasks are a viable product and manufacturers of PCM incorporated facemasks could use CFD to prototype PCM incorporated cotton facemasks at different environmental conditions and windspeed without needing to create a physical model which would cost capital and time.

References

- [1] Hassi, J., Rytönen, M., Kotaniemi, J., & Rintamäki, H. (2005). Impacts of cold climate on human heat balance, performance and health in circumpolar areas. *Int J Circumpolar Health*, 64(5), 459-467.
- [2] Budd, G. M. (1993). Cold stress and cold adaptation. *Journal of Thermal Biology*, 18(5), 629-631.
- [3] Gavhed, D. C. E., & Holmér, I. (1998). Thermal responses at three low ambient temperatures: Validation of the duration limited exposure index. *International Journal of Industrial Ergonomics*, 21(6), 465-474.

- [4] Ole Fanger, P. (2001). Human requirements in future air-conditioned environments. *International Journal of Refrigeration*, 24(2), 148-153.
- [5] Habchi, C., Ghali, K., & Ghaddar, N. (2014). Improved thermal performance of face mask using phase change material. *Textile Research Journal*, 84(8), 854-870.
- [6] Defence, Medicine, C. I. o. E., & Ducharme, M. (1999). *Benefits of respiratory heat and moisture exchangers during cold exposures*. Defence and Civil Institute of Environmental Medicine.
- [7] Feng, S., Shen, C., Xia, N., Song, W., Fan, M., & Cowling, B. J. (2020). Rational use of face masks in the COVID-19 pandemic. *Lancet Respir Med*, 8(5), 434-436.
- [8] Wei, L., English, A. S., Talhelm, T., Li, X., Zhang, X., & Wang, S. People in Tight Cultures and Tight Situations Wear Masks More: Evidence From Three Large-Scale Studies in China. *Personality and Social Psychology Bulletin*, 0(0), 01461672231210451.
- [9] Konda, A., Prakash, A., Moss, G. A., Schmoldt, M., Grant, G. D., & Guha, S. (2020). Aerosol Filtration Efficiency of Common Fabrics Used in Respiratory Cloth Masks. *ACS Nano*, 14(5), 6339-6347.
- [10] Mondal, S. (2008). Phase change materials for smart textiles – An overview. *Applied Thermal Engineering*, 28(11), 1536-1550.
- [11] He, B., & Setterwall, F. (2002). Technical grade paraffin waxes as phase change materials for cool thermal storage and cool storage systems capital cost estimation. *Energy Conversion and Management*, 43(13), 1709-1723.
- [12] Ghali, K., Ghaddar, N., Harathani, J., & Jones, B. (2004). Experimental and Numerical Investigation of the Effect of Phase Change Materials on Clothing During Periodic Ventilation. *Textile Research Journal*, 74(3), 205-214.
- [13] Hossain, M. T., Shahid, M. A., Ali, M. Y., Saha, S., Jamal, M. S. I., & Habib, A. (2023). Fabrications, Classifications, and Environmental Impact of PCM-Incorporated Textiles: Current State and Future Outlook. *ACS Omega*, 8(48), 45164-
- [14] Liu, Y., Liu, L., Li, Z., Zhao, Y., Liu, J., & Yao, J. (2019). 3D network structure and sensing performance of woven fabric as promising flexible strain sensor. *SN Applied Sciences*, 2(1), 70.
- [15] Dbouk, T., & Drikakis, D. (2020). On respiratory droplets and face masks. *Phys Fluids* (1994), 32(6), 063303.